Multi-Step FRET-Based Long-Range Nanoscale Communication Channel

Murat Kuscu, *Student Member, IEEE* and Ozgur B. Akan, *Senior Member, IEEE*

***Abstract*—Nanoscale communication based on Förster Resonance Energy Transfer (FRET) is a promising paradigm that allows future molecular-size machines to communicate with each other over distances up to 10 nm using the excited state energies of fluorescent molecules. In this study, we propose a novel nanoscale communication method based on multi-step FRET using identical fluorophores as relay nodes between communicating nanomachines, and utilizing multi-exciton transmission scheme in order to improve the limited range of the communication and achievable transmission rate over the nanoscale channel. We investigate two communication scenarios: immobile nanomachines communicating through a channel in a host material with linearly located relay nodes, and mobile nanomachines communicating through a channel in a 3-dimensional aqueous environment with randomly deployed relay nodes. We simulate the communication over these channels with realistic algorithms considering the high degree of randomness intrinsic to FRET phenomenon. Using the simulation results and following a Monte Carlo approach, we evaluate the performance of the channels by means of information theoretical capacity and interference probability. We show that multi-step FRET-based communication significantly outperforms the other biologically inspired nanocommunication techniques proposed so far in terms of maximum achievable data transmission rates. The results underline the compatibility and practicality of the FRET-based communication for several applications ranging from molecular computers to nanosensor networks.**

***Index Terms*—Multi-step FRET, nanoscale communications, fluorophores, nanonetworks, zeolite L, channel capacity, achievable rate, drug delivery, cancer treatment, nanosensor networks.**

I. Introduction

RECENT developments in nanotechnology have enabled manufacturing of low-power and low-cost molecular-size machines, i.e., nanomachines, with the most basic sensing, actuating and computing capabilities by the manipulation of molecules at individual level. The limited coverage and functionalities of nanomachines can be improved significantly with the development of intra- and inter-communication systems for these tiny machines. A group of nanomachines cooperatively exchanging some sort of information is envisioned as *nanonetwork*. The coordination of nanomachines with various capabilities in nanonetworks is envisaged to enable cutting-edge applications including healthcare monitoring, in-body drug delivery and nuclear defence [1].

The authors are with the Next-generation and Wireless Communications Laboratory (NWCL), Department of Electrical and Electronics Engineering, Koc University, Istanbul, 34450, Turkey (e-mail: {mkuscu, akan}@ku.edu.tr).

This work was supported in part by the Turkish Scientific and Technical Research Council under grant #109E257, by the Turkish National Academy of Sciences Distinguished Young Scientist Award Program (TUBA-GEBIP), and by IBM through IBM Faculty Award.

Many research efforts have been directed toward the development of a communication system between nanomachines. While some of the studies concentrate on the adaptation of traditional communication systems to nanoscale, e.g., electromagnetic [2], acoustic [3] communications, some of them are inspired by nature and imitate the biological communication systems for their models. Examples of biologically inspired models include the systems based on gap junction channels [4], as well as pollens and spores [5]. The majority of the efforts have been devoted to the molecular communications that use the molecules to encode and transfer the information [6]. Recently, we have proposed a novel and radically different molecular communication method based on a well-studied phenomenon FRET [7], [8].

FRET is the non-radiative transfer of excited state energies between two fluorescent molecules, i.e., fluorophores, such as fluorescent proteins, organic dyes, and semiconductor nanoparticles, e.g., Quantum Dots (QD) [9]. It is a quantum mechanical phenomenon based on the dipole-dipole interactions of the flurophores [10], and observed in some biological systems, such as photosynthesis [11]. It is a pairwise energy transfer between an excited donor fluorophore and a ground-state acceptor fluorophore. Basically, FRET requires three conditions to be satisfied: (i) spectral similarity of the fluorophores, i.e., the emission spectrum of the donor and the absorption spectrum of the acceptor must sufficiently overlap; (ii) proximity of the fluorophores, i.e., the donor and the acceptor must be in close proximity such as 0-10 nm; (iii) non-orthogonality of the transition dipole moments of the donor and the acceptor. If these conditions are satisfied, the donor transfers its excited state energy to a nearby acceptor when it is excited by a stimulus.

In [8], we have modeled the FRET-based communication channel between a single Transmitter-Receiver Nanomachine (TN-RN) pair and analyzed its information theoretical capacity. In that study, utilizing binary On-Off Keying (OOK) modulation, the information is encoded into two bits: bit-1 and bit-0. Bit-1 is represented by the transfer of a single exciton from the excited donor on TN to the ground-state acceptor on RN that is in the close proximity of TN, and bit-0 is represented as silence during a bit interval. In that study, we also investigate the effects of some environmental and intrinsic parameters of fluorophores on the channel capacity, and underline the strong dependence of the capacity on the distance between TN and RN. This dependence strongly reduces the reliability of the communication for internodal distances over 10 nm, and thus confines its practicality to very limited applications.

In this study, we propose a novel method for FRET commu-

nication based on multi-step FRET employing identical relay fluorophores between TN and RN, and utilizing multi-exciton transmission scheme in order to improve the spatial range and the achievable transmission rate of the communication. We investigate two deployment scenarios for the relay fluorophores: ordered relays in a host material with prescribed locations, and disordered, i.e., randomly deployed, relays in a three dimensional aqueous medium. The channel with ordered relays is considered for immobile nanomachines communicating through a wire-like channel that can find practicality for several on-chip applications. The channel with randomly deployed relays is considered for mobile nanomachines that can constitute mobile ad-hoc nanonetworks and nanosensor networks. We simulate the communication through the proposed channels following a realistic algorithm based on the competitive behavior of the multiple excitons and concerning many sources of randomness intrinsic to the phenomenon. Following a Monte Carlo approach, we evaluate the performance of the channels by means of information theoretical capacity and interference probability between successive transmissions, then we derive the maximum achievable data transmission rates over these channels. We infer from the results that using the channels with both ordered and disordered relays, two nanomachines can communicate at a rate up to tens of Mbps through distances over tens of nanometers. To the best of our knowledge, the achievable rates with multi-step FRET-based communication over this range of distances are significantly higher than that can be achieved by any biologically inspired communication method proposed so far.

The remainder of this paper is organized as follows. In Section II, we explain the basic principles of multi-step FRET-based nanocommunications and excitonic processes. In Section III and IV, we model the point-to-point multi-step FRET-based communication channels with ordered and randomly deployed relay fluorophores. The proposed channels are information theoretically analyzed, and the achievable rates are derived in Section V. In Section VI and VII, we discuss the networking capabilities and possible applications of FRET-based nanocommunications. Finally, the concluding remarks are given in Section VIII.

II. Multi-Step FRET-Based Communications

Multi-step FRET defines the sequential transfer of excitons, i.e., excited state of fluorophores, through more than one fluorophore. The excitons generated on the donor and transferred to the acceptor molecule might be transferred to another fluorophore that is spectrally similar and spatially proximal to the acceptor. Multi-step FRET has been studied extensively in order to improve the spatial range of FRET over 10 nm [12]. Based on the multi-step FRET, we have recently modeled a communication channel for a TN-RN pair with a single additional relay node (HN) located in the middle of them comprising a fluorophore which is spectrally similar to both the donor on TN and the acceptor on RN [8]. In that basic model, the nodes are located in a linear arrangement, and utilizing ON-OFF Keying (OOK) modulation IS sends a picosecond-duration pulse to TN in order to represent bit-1. We have shown that the channels TN-HN and HN-RN are independent with the proper selection of the bit interval T_b. Therefore, the overall transition probabilities between TN and RN are just the multiplication of the transition probabilities of each of the channel that participates in the communication.

Here, we extend our model employing multiple identical fluorophores as relay nodes between TN and RN, and utilizing multi-exciton transmission with ns-duration pulses.

A. Communication System Model

The multi-step FRET-based nanoscale communication system is composed of four main parts similar to traditional communication systems: an Information Source (IS), a transmitter nanomachine, a communication channel, and a receiver nanomachine:

- ***Information Source:*** The main information source of the system can be an external excitation source such as commercial laser that aims to remotely control the operation of a nanonetwork by sending optical pulses to TN. It might also be an electrical source that is embedded onto TN in the case semiconductor nanomaterials are used on TN as donor molecules. Utilizing OOK modulation, the information is encoded into two bits: bit-1 and bit-0. We assume that IS sends optical or electrical excitation pulses to TN with T_{pulse}-duration at the beginning of a bit interval T_b in order to represent bit-1, and keeps TN silent during T_b to represent bit-0.
- ***Transmitter Nanomachine:*** The transmitter with molecular sizes includes a donor molecule that receives the excitation pulses from IS and generates excitons. The emission spectrum of the donor molecule is assumed to overlap with the absorption spectra of the relay fluorophores, and the donor is assumed to be in close proximity of the relays, such that, the transfer of the generated excitons from the donor to the relay fluorophores is possible. On the contrary, we neglect the back transfer of the excitons from the relay fluorophores to the donor assuming the emission spectra of the relays and the absorption spectrum of the donor do not overlap.
- ***Communication Channel:*** For the communication channel, we investigate two basic cases. For the first case, the relay fluorophores are located on prescribed locations with prescribed orientations throughout a zeolite L backbone. The communication between TN and RN located on the different ends of zeolite L is realized through the wire-like structure with sequential energy transfers. In the second case, the relay fluorophores are randomly located and oriented in a three dimensional virtual lattice over aqueous medium and assumed to undergo random movements following Brownian statistics. In both cases, the excitons are transferred between the identical relay fluorophores via homoFRET. The underlying mechanism of homoFRET is the same as the one of FRET, except that it occurs between identical molecules, therefore, it requires that the emission and absorption spectra of the employed molecules must have a significant overlap.
- ***Receiver Nanomachine:*** The receiver includes an acceptor fluorophore that is the final destination of the excitons.

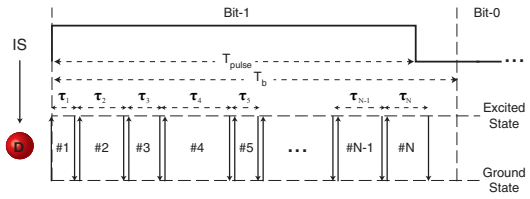

Fig. 1. Representation of bit-1 and bit-0 by IS, and sequential generation of N excitons on Donor (D) with random inter-generation times.

The absorption spectrum of the acceptor and the emission spectra of the relays are assumed to overlap. However, the emission spectrum of the acceptor and the absorption spectra of the relays do not overlap in order to avoid back transfer from the acceptor to the relays. The receiver is assumed to be synchronized with TN and continuously senses the state of the acceptor. We assume that the detection is realized by an external or internal photon detector. When the acceptor is excited via FRET during T_b, it releases a photon that is detected by the photon detector, and RN decides bit-1. If the photon detector does not detect any photon with a wavelength that is belong to the emission spectrum of the acceptor during the bit interval, RN decides bit-0.

Since we focus on the communication channel characteristics, the design of the transmitter and receiver nanomachines is out of the scope of this paper.

B. Principles of Exciton Activity

During the transmission of bit-1, the generated excitons occupy fluorophores for a random time, then they are transferred to another fluorophore via FRET or removed from the system via fluorescence. These processes are detailed as follows:

- ***Exciton generation:*** When IS sends an excitation pulse to TN, the donor is immediately excited, i.e., it generates an exciton, assuming the absorption coefficient of the donor is 1. Once the exciton is generated, it stays on the donor for a random time, then the donor relaxes through either fluorescence or FRET. In the case of FRET, the generated exciton is transferred to a proximal fluorophore. If T_{pulse} is large enough, after the first relaxation, the donor is expected to undergo many excitation and relaxation cycles during T_{pulse}, i.e., we expect more than one exciton to be generated by one pulse as demonstrated in Fig. 1. However, the number of generated excitons by a single pulse is a random variable, since the inter-generation times, i.e., the occupation times of generated excitons on donor, are random.
- ***Exciton occupation:*** An exciton occupies a fluorophore when it is generated on or transferred to that molecule. An occupied fluorophore is not available for the occupation of another exciton until it relaxes. The interval between the excitation and the relaxation of a fluorophore τ gives the occupation time of that exciton. τ is an exponential random variable with a mean μ_τ which depends on the FRET rate of the donor molecule to the proximal and available, i.e., ground-state, fluorophores, and the intrinsic lifetime of the donor molecule. Assuming there are k fluorophores available for energy transfer in the range of the donor, the mean occupation time of the ith exciton can be expressed in terms of the process rates:

$$\mu_{\tau_i} = (k_R + \sum_{j=1}^{k} k_{T,j,i})^{-1} \tag{1}$$

where $k_{T,j,i}$ is the FRET rate between the excited fluorophore and the jth proximal fluorophore for the ith exciton. k_R is the intrinsic fluorescence rate of the excited fluorophore. $k_{T,j,i}$ depends on intrinsic and environmental parameters [9] and can be expressed by:

$$k_{T,j,i} = 8.8 \times 10^{22} \kappa_{j,i}^2 n^{-4} J_j(\lambda) \frac{k_R}{R_{j,i}^6} \tag{2}$$

where $\kappa_{j,i}^2$ is the orientation factor which is a measure of the relative orientation of the transition dipole moments of the occupied and the jth proximal fluorophore during the occupation of the ith exciton. J_j is the degree of the spectral overlap between the emission spectrum of the occupied fluorophore and the absorption spectrum of the jth proximal fluorophore. $R_{j,i}$ is the intermolecular distance between the occupied fluorophore and the jth proximal fluorophore for the occupation time of the ith exciton.

- ***Exciton transfer:*** After a random occupation time, the exciton leaves the fluorophore by either fluorescence or FRET to another proximal fluorophore. The exciton randomly selects the next pathway from a set of possible pathways. Assuming that k proximal fluorophores are available for the energy transfer, the probability of FRET to a specific fluorophore can be expressed by

$$P_{FRET,j,i} = \frac{k_{T,j,i}}{k_R + \sum_{l=1}^{k} k_{T,l,i}} \tag{3}$$

- ***Exciton removal:*** An exciton is removed from the system by exciton recombination, i.e., the recombination of electron and hole. The prevalent recombination mechanism among dyes and fluorescent proteins is radiative recombination that results in radiation of a photon. The excitonic energy is converted to a photon with a wavelength dependent on the emission spectrum of the occupied fluorophore. For an exciton that occupies a fluorophore with k available neighbor fluorophores, the probability of fluorescence is given as

$$P_{Fluo,i} = \frac{k_R}{k_R + \sum_{l=1}^{k} k_{T,l,i}} \tag{4}$$

The excitons generated on TN are expected to move following random pathways through the relay nodes that surround both TN and RN. The overall movement of the excitons can be described as continuous-time correlated random walk with waiting times. Both the probability mass function (pmf) of the next jump, i.e., transition probabilities, and the waiting times on each node depend on the location, orientation and the availability of the surrounding fluorophores. Therefore, the

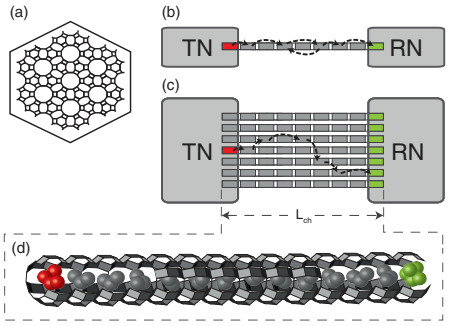

Fig. 2. (a) Hexagonal structure of zeolite L with seven channels. (b)-(c) 2-dimensional demonstration of multi-step FRET-based communication with relay nodes placed through a single zeolite L channel and seven zeolite L channel. (d) Detailed demonstration of a single zeolite L channel filled up with donor (red), relay (gray) and acceptor (green) fluorophores.

next jump of an exciton is independent of the previous jumps, however, it depends on the trajectories of other excitons that might simultaneously exist in the channel. The excitons that exist in the channel at the same time compete with each other to occupy the available fluorophores.

III. Multi-Step FRET-Based Communication Channel with Ordered Relays

Here, we investigate two FRET-based long-range communication channels with identical relay fluorophores placed in prescribed locations. For the immobility of the fluorophores, we assume a host material zeolite L is employed.

Zeolite L has a porous molecular structure and is composed of strictly parallel channels formed by the combination of these pores in a hexagonal arrangement as demonstrated in Fig. 2(a). The free diameter inside the channels is 0.71 nm and the length of the channels ranges from 30 nm up to 10 μm [13]. Also the center-to-center distance between two parallel channels is 1.84 nm [13]. The dimensions of the channels make it possible to fill these zeolite L channels up with several well-oriented dye molecules. Zeolite L is an advantageous host material for fluorescent dyes because of its negatively charged framework [14]. Unidirectional energy transfer from an energy source to a reaction center through the zeolite L channels filled up with guest molecules, e.g. fluorescent dyes, are extensively studied especially for light harvesting applications, e.g. artificial antenna systems, [13], [15]. In most of the studies, the same kind of dye molecules are employed between two ends of the channels as relay nodes and the excited energy is transferred via homoFRET.

We focus on two basic models. In the first model, the relay fluorophores are placed in a single zeolite L channel, such that they are arranged in a single axis as seen in Fig. 2(b). The transition dipole moments of each fluorophore are assumed to be parallel to the common axis. Therefore, the relative orientation factor is maximized, i.e., $\kappa^2 = 4$, which significantly increases the probability of FRET through relay fluorophores. In this communication scheme, TN and RN are assumed to be immobile connected to different ends of the zeolite L channel as in Fig. 2(b). The connection can be established mechanically or covalently through the connector molecules that are employed both on the nanomachines and at the channel ends. We assume the intermolecular distance between the donor and the first relay, as well as between the acceptor and the last relay, is 2 nm which is the spacing between two neighboring pores. We also assume that none of the pores are empty, therefore, the inter-relay distance is also 2 nm. The donor and the acceptor which are the antennas of the nanomachines exchange the excited energy, i.e., excitons, with neighboring relay fluorophores through the FRET mechanism.

For the second model, we utilize seven parallel zeolite L channels in a hexagonal arrangement as the host for fluorophores. A donor molecule is located at one end of the channel in the middle, and seven acceptor molecules are located at the other end of seven channels as shown in Fig. 2(c). The rest of the channels are filled up with relay molecules uniformly such that each of the unit cells in the channel is occupied by a relay, therefore, the center-to-center distance between two adjacent fluorophores in the same channel is 2 nm. We assume that the donor molecule can be excited directly by an optical or electrical pulse with the duration in the range of nanoseconds that is sent from an information source that can be external or internally embedded onto TN. The excited donor is relaxed through either fluorescence or FRET to one of the relay molecules in its range with different probabilities. All of the molecules are oriented parallel to the channel axes. Considering the fluorophores located in different parallel channels, the orientation factor for any pair of fluorophores is expressed by $\kappa^2 = (1 - 3\cos^2\theta)^2$, where θ is the angle between the channel axis and the virtual axis that connects the center of both fluorophores [9]. RN is assumed to continuously observe all of the acceptors' states such that if at least one of the acceptors fluoresces in the bit interval, it decides that bit-1 is transmitted.

Since we employ identical relays throughout the channel for both models, it is possible for an exciton occupied on a relay to be transferred in all of the directions: in the direction of the donor end, or the acceptor end. Moreover, for the seven-channel model, excitons can be exchanged between the fluorophores in the different parallel channels of zeolite L. We assume that relay emission band and donor absorption band, as well as, acceptor emission band and relay absorption band do not overlap, therefore, we neglect FRET from a relay to the donor, and from an acceptor to a relay.

IV. Multi-Step FRET-Based Communication Channel with Disordered Relays

We consider another multi-step FRET based communication case comprising identical fluorophores located randomly in a 3-dimensional aqueous environment as seen in Fig. 3. The fluorophores are expected to move uniformly in each direction following Brownian statistics, therefore, at any time instant, the spatial distribution of the fluorophores is assumed to be uniform throughout the environment. Assuming isotropic and unrestricted distributions for all three angles, the individual relay fluorophores freely rotate. Following the assumption, the orientation factor for each pair of the relays is subject to the given probability density function [16]

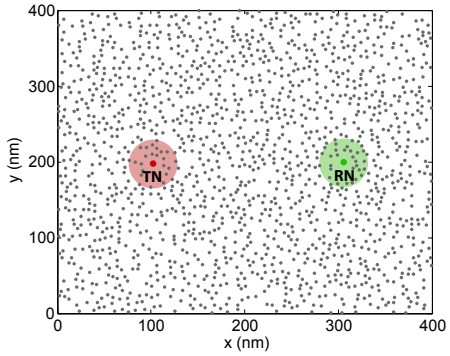

Fig. 3. Two dimensional demonstration of randomly deployed relays throughout the lattice surrounding TN and RN. The excitons released by TN undergo random jumps through the relay nodes, and some of them reach RN.

$$p_{\kappa^2}(\kappa^2) = \begin{cases} \frac{1}{2\sqrt{3\kappa^2}} \ln(2+\sqrt{3}) & 0 \leq \kappa^2 \leq 1 \\ \frac{1}{2\sqrt{3\kappa^2}} \ln\left(\frac{2+\sqrt{3}}{\sqrt{\kappa^2}+\sqrt{\kappa^2-1}}\right) & 1 \leq \kappa^2 \leq 4 \end{cases} \quad (5)$$

The donor, acceptor and relay fluorophores are considered as spherical molecules with diameter of 1.2 nm. There are just one donor and one acceptor in the considered lattice. The paper is not concerned with the design of transmitter and receiver nanomachines, therefore, we assume that, a single donor functions as TN which receives the information from a remote IS, and a single acceptor functions as RN which sends the received information to another remote observer through fluorescence. TN and RN are assumed to be mobile with controllable movements, therefore, they are not subject to Brownian statistics.

We assume that there is no collisional quencher which removes the excitons when it collides with an excited fluorophore. Therefore, there are only two processes that an exciton can undergo: fluorescence and FRET to a nearby fluorophore.

V. Information Theoretical Analysis

In this section, we analyze the information theoretical capacity of the aforementioned channels. Additionally, we investigate the interference between successively transmitted bits, and derive the maximum achievable data transmission rates for each channel in the case of OOK modulation.

For each communication system, we utilize the most basic modulation technique: binary OOK modulation with two bits available, bit-1 and bit-0. IS sends a T_{pulse}-duration optical or electrical pulse to TN at the beginning of a T_b-duration time slot in order for TN to transmit bit-1. For bit-0, IS does not send any pulse and keeps TN silent during T_b. Bit-1 is successfully transmitted if the acceptor on RN is excited in the relevant time slot. Bit-0 is transmitted successfully if the acceptor stays in ground-state during T_b.

Assuming there is no excitation-source except from IS, the transmission of bit-0 is always successful, i.e., $p_0 = 1$, if we neglect a probable ISI situation. However, the transmission of bit-1 is ambiguous because of the high degree of randomness and the correlated behavior in the motion of excitons. It is very difficult to derive an analytical solution for the successful transmission probability of bit-1, i.e., p_1. For that reason, we simulate the transmission of bit-1 in Matlab using a common algorithm for all the channel models. Following a Monte Carlo approach, we derive the successful transmission and ISI probabilities for different channel parameters.

Since the transmission of bit-1 is problematic and the transmission of bit-0 is always successful, information theoretically the channels show Z-channel characteristics [17]. Considering an input alphabet $\mathbf{X} = \{0,1\}$ which is transmitted by TN and an output alphabet $\mathbf{Y} = \{0,1\}$ which constitutes the set of received bits, and assuming that IS sends a pulse with probability P_1 and no-pulse with probability $1 - P_1$, the mutual information between the transmitted and received bits is expressed by $I(\mathbf{X};\mathbf{Y}) = H(P_1 \cdot p_1) - P_1 \cdot H(1 - p_1)$. Here, $H(.)$ is the binary entropy function. The capacity of the channel C is the maximum mutual information over all input distribution, i.e., $C = \max_{P_1} I(\mathbf{X};\mathbf{Y})$.

A. Simulation Algorithm

We conduct simulations for the transmission of bit-1 on each channel based on the algorithm demonstrated in Fig. 4. The channel parameters used in the simulations for ordered and disordered cases are given in Table I-II. Here, the Förster radius is the intermolecular distance when the FRET probability is 0.5, i.e., when the FRET rate is equal to the fluorescence rate for single pair of fluorophores. It is a measure of the spatial range of FRET, such that, for intermolecular distances greater than $2R_0$, the probability of FRET is negligible because of the sixth power dependence on distance. That is why we set the transfer range of the excitons to $2R_0$. The exciton transfer over distances greater than the transfer range is neglected in the simulations. Depending on the environmental parameters, R_0 ranges from 2 nm to 7 nm for common fluorophores [9].

TABLE I
Simulation Parameters (Ordered Relays)

Förster radius (R_0)	4 nm
Pulse length (T_{pulse})	$10, 50, 100, 500$ ns
Channel length (L_{ch})	$30 - 134$ nm
Number of zeolite L channels	$1, 7$
Fluorescence rates (k_D, k_R, k_A)	5×10^8 1/s
Molecular radius (r)	1.2 nm
Transfer range	$2 \times R_0 = 8$ nm

TABLE II
Simulation Parameters (Disordered Relays)

Förster radius (R_0)	$3 - 7$ nm
Pulse length (T_{pulse})	$10, 50, 100, 500$ ns
Lattice size	$400 \times 400 \times 400$ nm
TN location	$(100, 100, 100)$ nm
RN location	$(103, 100, 100) - (301, 100, 100)$ nm
Relay concentration (M)	$480, 960, 1920$ mol/m^3
Fluorescence rates (k_D, k_R, k_A)	5×10^8 1/s
Molecular radius (r)	1.2 nm
Transfer range	$2 \times R_0$

The fluorescence rate is another key parameter for fluorophores. It is the reciprocal of the mean lifetime of fluorophores when there is no proximal acceptor and quencher.

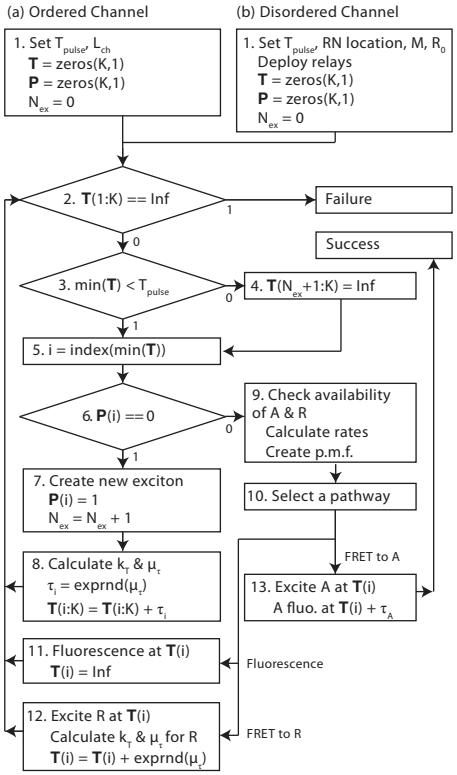

Fig. 4. Monte Carlo algorithm for the simulation of bit-1 transmission through the channels with (a) ordered and (b) disordered relays.

The mean lifetime ranges from picoseconds to tens of nanoseconds for common fluorophores [9]. We use a typical value of 2 ns for fluorescent dyes. Therefore, the fluorescence rate is assumed to be 5×10^8 1/s.

The algorithm used in each channel simulation is based on the competitive behavior of the excitons, and operates through the following steps:

1) The channel parameters are set. A time matrix $\mathbf{T}$ holding the last active time of each exciton in each row according to the indices of the excitons, and a state matrix $\mathbf{P}$ holding the state of each exciton are generated with K rows. K is set arbitrarily concerning that it has to be greater than the possible number of the excitons created in one transmission cycle. All of the rows of both matrices are set to 0 prior to the transmission. Once the exciton is created with index i on the donor, $\mathbf{P(i)}$ is set to 1. If the ith exciton is removed from the system, $\mathbf{T(i)}$ is set to an infinite value, i.e., $\mathbf{Inf}$.
2) The algorithm checks whether all the excitons are removed from the system. If there remains no active exciton, simulation ends with failure, otherwise it continues at Step 3.
3) The algorithm checks whether there is an exciton with the active time is less than T_{pulse}.
4) If the active times of all the excitons become greater than T_{pulse}, it means that the pulse ends, and no more excitons can be generated on the donor. Therefore, all of the inactive excitons are removed from the system by setting the time entries to $\mathbf{Inf}$. The simulation continues at Step 5 playing the already-activated excitons.
5) i is set to the index of the exciton with the minimum active time.
6) The algorithm checks whether the ith exciton has been generated before.
7) Exciton i is generated, i.e., activated. The number of generated excitons, i.e., N_{ex}, is incremented by 1.
8) The FRET rates k_T between the donor and each relay or acceptor molecules in the range of the donor are calculated considering the intermolecular distance and the relative orientations. μ_τ is calculated using (1). The excited state lifetime τ_i is determined randomly from the exponential distribution with mean μ_τ. Exciton i stays at the donor for a time τ_i. The time entries for the exciton i and for the excitons which have not been generated yet are incremented by τ_i, since the donor is not available until this time for the new excitons to be generated. The simulation continues at Step 2.
9) If the exciton i is already activated, the algorithm checks the available molecules for FRET at time $\mathbf{T(i)}$ and creates p.m.f. for the next pathway calculating the process rates.
10) A new pathway for the exciton i is selected randomly according to the p.m.f.
11) If exciton i results in fluorescence at time $\mathbf{T(i)}$, it is removed from the system by setting $\mathbf{T(i)} = \mathbf{Inf}$. The occupied molecule is relaxed and becomes available for the new excitons. The simulation continues at Step 2.
12) If exciton i occupies a relay molecule through FRET, the process rates are calculated checking the available molecules at time $\mathbf{T(i)}$. μ_τ is calculated accordingly. The exciton i stays at the relay molecule for a time τ_i which is determined randomly from the exponential distribution with mean μ_τ. The simulation continues with Step 2.
13) If exciton i is transferred to an acceptor molecule at time $\mathbf{T(i)}$, receiver detects bit-1 when the acceptor fluoresces at time $\mathbf{T(i)}+\tau_\mathbf{A}$. Since, the only way for the acceptors to relax is to fluorescence, τ_A is determined randomly from the exponential distribution with mean μ_{τ_A} regardless of the available molecules in the range. The simulation ends with the successful transmission of bit-1.

B. Analysis of Channels with Ordered Relays

The simulation of the transmission of bit-1 for the zeolite L channel models is run many times for different parameters. The success probability of bit-1 transmission p_1 is obtained as the number of successful transmissions divided by the total number of runs. The simulations are repeated until the obtained value of p_1 converges to a finite value, then, the channel capacity is derived information theoretically.

1) Single Zeolite L Channel Case: Fig. 5(a) demonstrates the information theoretical capacity of the communication channel constructed on a single zeolite L channel for different values of T_{pulse} with varying channel length L_{ch}. For the capacity analysis, we assume that the bit interval T_b is sufficiently large to neglect ISI. We investigate the ISI situation

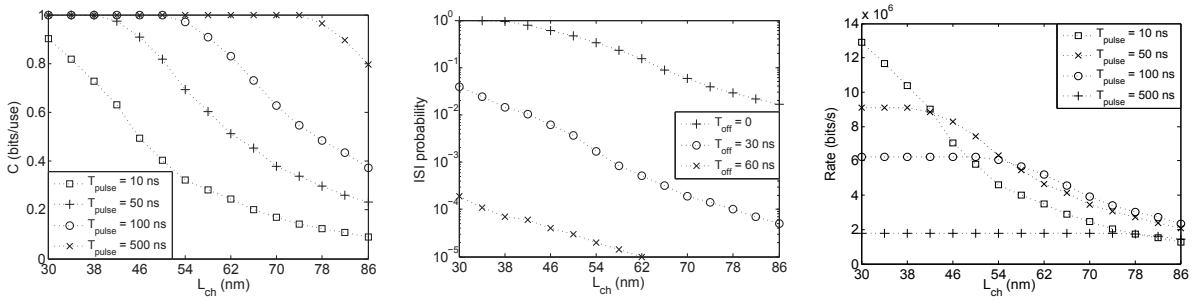

(a) Capacity for different pulse lengths with varying L_{ch}. (b) ISI probability for different offset times with varying L_{ch} and $T_{pulse} = 50$ ns. (c) Maximum achievable transmission rates for different pulse lengths with varying L_{ch}.

Fig. 5. Results of performance analysis for ordered channel with single zeolite L channel.

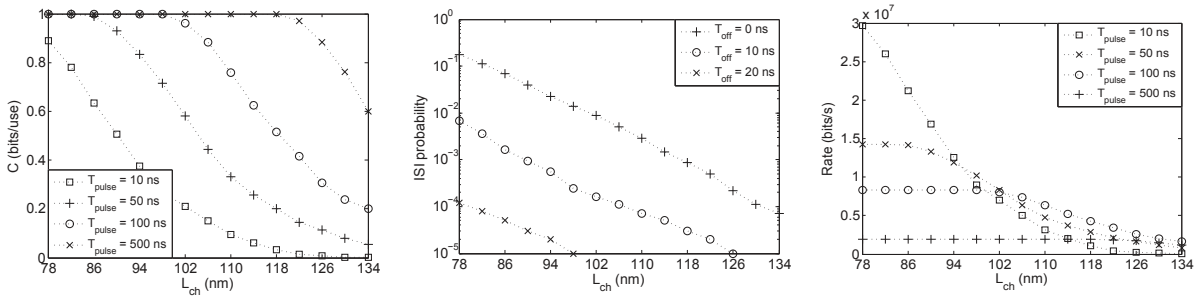

(a) Capacity for different pulse lengths with varying L_{ch}. (b) ISI probability for different offset times with varying L_{ch} and $T_{pulse} = 50$ ns. (c) Maximum achievable transmission rates for different pulse lengths with varying L_{ch}.

Fig. 6. Results of performance analysis for ordered channel with seven zeolite L channels.

in the next analysis. As is seen from Fig. 5(a), increasing the pulse length significantly improves the channel capacity, since as we increase T_{pulse}, more excitons are generated and the probability of error for bit-1 transmission decreases. At some critical channel length, the capacity of the channel starts to decrease. The critical channel length is larger for greater T_{pulse} values. Compared to the single-pair single-exciton FRET-based communication channel [8], the capacity and the range of the communication are significantly improved.

The main reason of InterSymbol Interference (ISI) is the excitons that are generated during a bit interval with duration T_b, and arrive to the receiver at a greater time than T_b. ISI makes ambiguous the detection of bit-0 in the case of a preceding bit-1 transmission. Due to the stochastic behavior of the exciton motion, it is not possible to completely avoid ISI, however, one can set a threshold for the bit interval in order to bring the ISI probability down to negligible values. The time-based characteristics of the channels related to ISI are investigated recording the removal times of the last excitons which are able to reach the receiver. The simulation results show that the variation in T_{pulse} only changes the mean removal time in proportion to T_{pulse}, and has negligible effect on the variance of the distribution. This is due to the fact that only the lastly generated excitons contribute to the late arrivals, therefore, the distribution of last arrival times is independent of the pulse length. Besides, altering the channel length L_{ch} substantially effects both mean and variance of the distribution. Therefore, we conduct ISI probability analysis by setting T_{pulse} to a constant value of 50 ns, and $T_b = T_{pulse} + T_{off}$, and varying L_{ch} and T_{off}. From the results demonstrated in Fig. 5(b), we conclude that setting $T_b = T_{pulse} + 60$ ns results in negligible ISI for the typical channel lengths.

The maximum achievable rates are given by $R_a = C/T_b$. Setting $T_{off} = 60$ ns for all T_{pulse} values, R_a with varying channel length is demonstrated in Fig. 5(c). We conclude that, two nanomachines can communicate reliably at a rate over 12 Mbps through a distance up to 30 nm, and over 2 Mbps through distances larger than 80 nm.

2) Seven Zeolite L Channel Case: The analyzes are repeated for the communication channel which includes seven parallel zeolite L channels as the host for fluorophores. The variation of the channel capacity for varying pulse and channel length is shown in Fig. 6(a). As seen from the figure, the spatial range of the communication is increased as approximately 40 nm compared to the channel composed of one zeolite L channel, i.e., the same capacity can be obtained at a distance 40 nm larger as compared to the single channel case. One of the reasons of this significant increase is that seven acceptor fluorophores are employed at RN. Locating more acceptors at RN, we increase the probability of exciton reception. The other reason is the increased number of proximal fluorophores for each fluorophore which reduces the fluorescence, i.e., removal, probability of excitons during the transmission.

The ISI case for seven zeolite L channel is investigated as in the case of one zeolite L channel. Setting $T_b = T_{pulse} + T_{off}$ and $T_{pulse} = 50$ ns, the probability of ISI for varying channel length is plotted in Fig. 6(b). Here, we see that as compared to the single channel case, smaller offset value is sufficient to

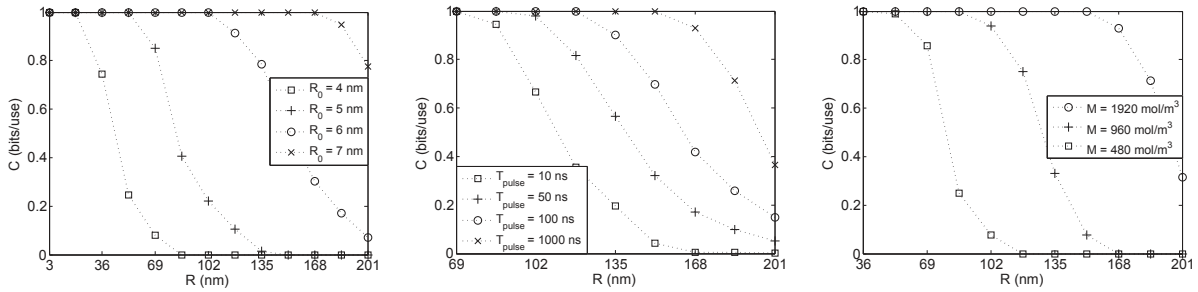

(a) Capacity for $M = 1920$ mol/m^3, $T_{pulse} = 1000$ ns, and varying R_0.

(b) Capacity for $M = 1920$ mol/m^3, $R_0 = 6$ nm, and varying T_{pulse}.

(c) Capacity for $T_{pulse} = 1000$ mol/m^3, $R_0 = 6$ nm, and varying M.

Fig. 7. Information theoretical capacity of disordered channel for different channel parameters with varying TN-RN distance R.

get negligible ISI. Setting $T_{off} = 20$ ns and neglecting ISI, the achievable rates are derived for different T_{pulse}, and the results are plotted in Fig. 6(c). Here, we conclude that with a channel composed of seven zeolite L channels with ordered relays, nanomachines can reliably communicate at a rate up to 30 Mbps over a distance up to 80 nm, and at a rate over 2 Mbps through a distance up to 130 nm. Compared to the single zeolite L channel case, the achievable rates are significantly improved.

C. Analysis of Channel with Disordered Relays

Here, we investigate the capacity of the disordered channel. The transmission probability of bit-1 is simulated following the algorithm described in Fig. 4, and using the parameters given in Table II. The simulations are repeated until p_1 converges to a finite value. Note that, for each run of the simulation, the relay fluorophores are deployed again in random locations following a uniform distribution. In the deployment stage, the algorithm takes the molecular sizes into account, such that, the Euclidean distance between the centers of two fluorophores cannot be smaller than $2r$, i.e., 2.4 nm. Although the relay molecules undergo Brownian motion, the displacement of the molecules during the transfer does not damage the homogeneity of the spatial distribution, since the relays uniformly move in each direction. Additionally, the relative orientation of each pair of fluorophores is randomly selected according to the distribution given in (5) for each exciton occupation in order to imitate the isotropic and unrestricted rotations of fluorophores. Using the converged value of p_1, the capacity is derived as the maximum mutual information between the transmitted and received bits over all input distributions.

Setting the molar concentration of relay fluorophores in the environment as 1920 mol/m^3, and using excitation pulses with duration $T_{pulse} = 50$ ns to represent bit-1, the information theoretical capacity of the channel is plotted in Fig. 7(a) for different values of Förster distance and varying TN-RN distance R. The results show that R_0 has great effect on the spatial range of the communication, such that, using fluorophores with $R_0 = 7$ nm, TN and RN can communicate reliably over distances larger than 150 nm even with a comparatively low value of T_{pulse}.

The effect of the pulse length on the capacity is demonstrated in Fig. 7(b). Here, we set the molar concentration as $M = 1920$ mol/m^3, and use fluorophores with $R_0 = 6$ nm. As expected, increasing the pulse length, the capacity of the channel increases significantly.

Lastly, we investigate the effect of the relay concentration on the channel capacity. In Fig. 7(c), the capacity is plotted for three typical concentration values with varying distance between TN and RN. As is seen, increasing the molecular concentration improves the communication range. For relatively denser concentrations, an individual relay fluorophore has many available fluorophores in its proximity. As a result, the removal probability of excitons is comparatively low which increases the probability of exciton transmission from TN to RN for bit-1 case.

We investigate the ISI situation by running the simulation many times, and recording the removal times of excitons that lastly arrive to RN. Setting $T_{pulse} = 10$ ns and $T_b = T_{pulse} + T_{off}$, we plot the ISI probability for different time offsets with varying R and molecular concentration in Fig. 8(a). From the results, we conclude that adding a time offset of 2 ns to T_{pulse} reduces the ISI probability to negligible values. The required time offset for negligible ISI is very low compared to that of zeolite L based channels. Since, a relay fluorophore is surrounded by many available fluorophores in brownian channel, the mean occupation time of excitons on relay fluorophores decreases to very low values, e.g., 1-10 ps for very dense environments. As a result, the transit time of excitons from TN to RN is also reduced. The decrease in the ISI probability with increasing molecular concentration also justifies this reasoning.

Setting $T_{off} = 2$ ns and neglecting ISI, in Fig. 8(b), we plot the achievable rates with varying R. It is demonstrated that mobile TN and RN can communicate at a rate over 80 Mbps if they are in approximately 70 nm-proximity of each other, and with 200-nm proximity, the reliable communication can be realized at a rate over 1 Mbps.

VI. FRET-Based Nanonetworks

Excitons are randomly radiated to a relatively large area through sequential transfers. Therefore, there might be more than one RN in the range of TN, and we expect that all of RNs with the spectrally appropriate acceptor can receive

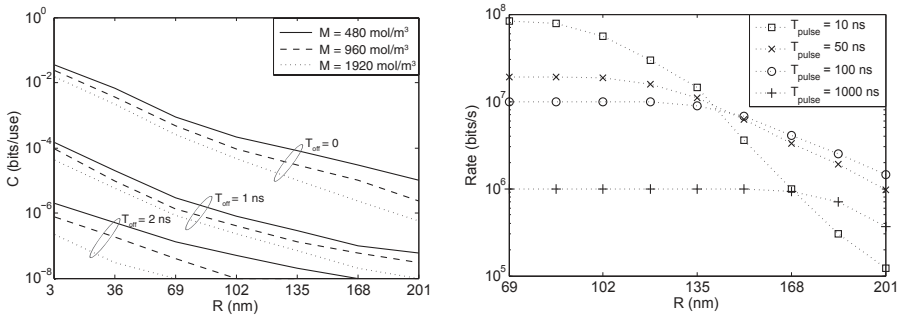

(a) ISI probability for disordered channel with varying T_{off}, M and R.

(b) Maximum achievable rate for disordered channel with varying T_{pulse} and R.

Fig. 8. Results of ISI and achievable rate analysis for disordered channel.

information from TN with a probability of error that is directly dependent on the Euclidian distance between TN and RN. The system is similar to traditional broadcast communication where a transmitter radiates electromagnetic signals in all directions without any knowledge about receivers. In electromagnetic case, receiver antenna has to be tuned to the carrier frequency to receive information from transmitter. Similarly, in FRET-based case, for RN to receive exciton signals, absorption spectrum of RN acceptor must overlap with the emission spectra of relay fluorophores, i.e., carrier fluorophores. Furthermore, the emission spectrum of TN donor must overlap with the absorption spectra of relays for the transfer of excitons into the channel.

Different TN-RN pairs can communicate through the same physical medium if a multiple-access method is utilized. For this aim, wavelength division multiplexing can be applied if another sort of relay fluorophore which spectrally does not overlap with the other relay is available in the medium. Accordingly, different donor and acceptor that overlap with the new relay must be employed on the second TN-RN pair, respectively, so that the second pair can communicate through the new relay fluorophores. The interference between these two channels depends on the separation of the optical spectra of the employed fluorophores. The spectral range of common fluorescent molecules is limited, therefore, in order to employ more channels in the same medium, fluorophores with narrow spectral widths, e.g., fluorescent dyes, must be preferred.

In [18], it is demonstrated that employing a semiconductor donor, e.g., QD or Quantum Rods (QR), TN can tune the emission spectrum of the donor electrically. Tuning the spectrum of the donor, TN can select the receiver nodes to communicate with if there are more than one sort of relay fluorophores in the channel as in the case of multiple-access.

VII. Applications

In this section, we discuss some prospective applications of FRET-based long-range communication. We do not go into detail about their physical realizations, but we relate our investigations as promising solutions to some open problems.

Nanomachines are expected to perform very basic tasks, such as simple logic operations, sensing, or actuating. The most important promise of a nanonetwork is to coordinate the nanomachines with different capabilities in order to perform more complex tasks and to increase the effective range of the operation combining these tiny machines deployed in relatively large area.

There is a large number of studies concerning the design of molecular machines some of which exploit the excitons to realize their functionalities [19]. For example, photoactive nanovalves and nanoimpellers that are activated with the excitation of functional fluorophores have been designed [20]. There are also several nanosensors employing fluorophores as functional unit in that the functional fluorophore becomes excited and then fluoresces when a target molecule bounds to them [21]. FRET-based communication promises a nanonetwork that combines the different functionalities of this kind of molecular machines without a need for additional complex processing or energy conversion units. Since the nanosensors output as excitons when they detect a target, and the molecular machines can actuate when they are activated by excitons, the communication between all these different nanomachines can be realized by the transfer of excitons, i.e., FRET-based communications. For example, consider a drug delivery task that needs a precise control of the location where the drugs are delivered. This need is important especially for cancer treatment, since the delivered drug might be harmful for healthy cells, and must be delivered precisely to the tumor cells. A nanonetwork composed of nanosensors that can detect the tumor cells, and nanoactuators, e.g., a combination of nanopores and nanovalves, that can release the drug molecules when it is activated by an exciton, might be a solution to this problem if the communication of the nanosensor with the nanoactuators is realized. FRET-based communication is the simplest and realizable option to connect these primitive molecular devices without additional complexity.

Another example about the cancer treatment is photodynamic therapy (PDT) that is based on the apoptosis of tumor cells by reactive singlet oxygen species. The singlet oxygen is generated when a photosensitizer agent is excited and transfers its excited energy to a nearby oxygen molecule. It has been shown that the photosensitizer agent also can be excited through FRET by designing a system with additional QD as the energy donor [22]. The system can be considered as the actuating unit in a nanonetwork composed of FRET-

based communicating nanosensors and other nanoactuators specialized in cancer treatment.

An FRET-based nano sensor network composed of many molecular sensors deployed in a large area can be employed to gain a spatial diversity increasing the detection area. The outputs of the molecular sensors can be gathered through FRET-based communication in a processing unit that might have a more complex structure as compared to the sensors. This kind of nanosensor network extends the resolution of molecular diagnostics to single-molecule level in a coordinated manner, and can find applications in the areas like water-quality control, nuclear defence [2].

We show that FRET-based communication provides high data transfer rates compared to other short-range communication techniques especially when we have the advantage of placing fluorophores at prescribed locations. Parallel to the advances in the molecular logic gates and memories based on photochromic fluorophores, FRET is a promising communication technique in nanoscale on-chip applications such as nanoprocessors. Furthermore, exploiting the quantum coherence behavior of the energy transfer, FRET-based communication can find applications in quantum computers.

VIII. Conclusion

We propose a novel nanoscale communication method based on multi-step FRET employing multiple excitons as the information carrier, and investigate different scenarios for immobile and mobile nanomachines considering that they communicate through the channels with ordered and disordered relay fluorophores, respectively. The simulation results of both scenarios demonstrate that with multi-step FRET-based communication, significantly high data transmission rates are achievable over extended distances up to tens of nanometers. Parallel to the advances in molecular logic gate architectures, multi-step FRET-based communication is a promising solution for molecular computers with its high transmission rates. Moreover, we underline the practicality of the FRET-based communication for mobile applications such as nanosensor networks for health monitoring and in-body drug delivery.

References

[1] I. F. Akyildiz, F. Brunetti, C. Blazquez, "Nanonetworks: A new communication paradigm," *Comput. Netw.,* vol. 52, no. 12, pp. 2260-2279, 2008.

[2] I. F. Akyildiz, M. J. Jornet, "Electromagnetic wireless nanosensor networks," *Nano Commun. Netw.,* vol. 1, no. 1, pp. 3-19, 2010.

[3] T. Hogg and R. A. Freitas, "Acoustic communication for medical nanorobots," *Nano Commun. Netw.,* vol. 3, no. 2, pp. 83-102, 2012.

[4] T. Nakano, T. Suda, T. Koujin, T. Haraguchi, Y. Hiraoka, "Molecular communication through gap junction channels," *Springer Trans. Comput. Syst. Biol. X*, vol. 5410, pp. 81-99, 2008.

[5] L. P. Giné, I. F. Akyildiz, "Molecular communication options for long range nanonetworks," *Comput. Netw.*, vol. 53, no. 16, pp. 27532766, 2009.

[6] B. Atakan, O. B. Akan, S. Balasubramaniam, "Body area nanonetworks with molecular communications in nanomedicine," *IEEE Commun. Mag.,* vol. 50, no. 1, pp. 2834, 2012.

[7] M. Kuscu, O. B. Akan, "A nanoscale communication channel with fluorescence resonance energy transfer (FRET)," *Proc. 1st IEEE Int. Workshop Molecular Nano Scale Commun./IEEE Conf. Comput. Commun. Workshops,* Shanghai, China, 2011, pp. 425-430.

[8] M. Kuscu, O. B. Akan, "A physical channel model and analysis for nanoscale molecular communications with Förster Resonance Energy Transfer (FRET)," *IEEE Trans. Nanotechnol.,* vol. 11, pp. 200-207, 2012.

[9] J. R. Lakowicz, *Principles of fluorescence spectroscopy,* 3rd ed., Baltimore, MD: Springer-Verlag, 2006.

[10] T. Förster, "Zwischenmolekulare energiewanderung und fluoreszenz", *Annalen der Physik,* vol. 437, pp. 55-75, 1948.

[11] T. Ritz, A. Damjanovic, K. Schulten, "The quantum physics of photosynthesis," *ChemPhysChem,* vol. 3, no. 3, pp. 243-248, 2002.

[12] M. Heilemann, P. Tinnefeld, G. S. Mosteiro, M. G. Parajo, N. F. Hulst, M. Sauer, "Multistep energy transfer in single molecular photonic wires," *J. Am. Chem. Soc.,* vol. 126, no. 21, pp. 6514-6515, 2004.

[13] G. Calzaferri, K. Lutkouskaya, "Mimicking the antenna system of green plants", *Photochem. Photobiol. Sci.,* vol. 7, no. 8, pp. 879-910, 2008.

[14] S. Ramachandra, Z. D. Popovic, K. C. Schuermann, F. Cucinotta, G. Calzaferri, L. De Cola, "Förster resonance energy transfer in quantum dotdye-loaded zeolite L nanoassemblies", *Small,* vol. 7, no. 10, pp. 1488-1494, 2011.

[15] M. Pauchard, A. Devaux, G. Calzaferri, "Dye-loaded zeolite L sandwiches as artificial antenna systems for light transport", *Chem. Eur. J.,* vol. 6, no. 18, pp. 3456-3470, 2000.

[16] D. Badali, C. C. Gradinaru, "The effect of Brownian motion of fluorescent probes on measuring nanoscale distances by Förster resonance energy transfer", *Journal of Chemical Physics,* vol. 134, no. 22, pp. 225102, 2011.

[17] T. M. Cover, J. A. Thomas, *Elements of information theory,* New York: Wiley, 1991.

[18] M. Kuscu, D. Malak, O. B. Akan, "An information theoretical analysis of broadcast networks and channel routing for FRET-based nanoscale communications," in *Proc. 2nd IEEE Int. Workshop Molecular Nano Scale Commun./IEEE Conf. Commun. Workshops,* Ottawa, Canada, 2012, pp. 6167-6171.

[19] V. Balzani, A. Credi, F. M. Raymo, J. F. Stoddart, "Artificial molecular machines," *Angew. Chem. Int. Ed.,* vol. 39, no. 19, pp. 3348-3391, 2000.

[20] J. Lu, E. Choi, F. Tamanoi, J. I. Zink, "Light-activated nanoimpeller-controlled drug release in cancer cells," *Small,* vol. 4, no. 4, pp. 421-426, 2008.

[21] I. L. Medintz, A. R. Clapp, H. Mattoussi, E. R. Goldman, B. Fisher, J. M. Mauro, "Self-assembled nanoscale biosensors based on quantum dot FRET donors," *Nature Materials,* vol. 2, pp. 630-638, 2003.

[22] A. C. S. Samia, X. Chen, C. Burda, "Semiconductor quantum dots for photodynamic therapy," *J. Am. Chem. Soc.,* vol. 125, no. 51, pp. 15736-15737, 2003.

Murat Kuscu [S'11] (mkuscu@ku.edu.tr) received his B.Sc. degree in electrical and electronics engineering from Middle East Technical University, Ankara, Turkey, in July 2011. He is currently a research assistant at the Next-generation and Wireless Communications Laboratory (NWCL) and pursuing his M.Sc. degree in electrical and electronics engineering at Koc University, Istanbul, Turkey. His current research interests include nano-scale and molecular communications.

Ozgur B. Akan [M'00-SM'07] (akan@ku.edu.tr) received his Ph.D. degree in electrical and computer engineering from the Broadband and Wireless Networking Laboratory, School of Electrical and Computer Engineering, Georgia Institute of Technology in 2004. He is currently a full professor with the Department of Electrical and Electronics Engineering, Koc University and the director of the Next-generation and Wireless Communications Laboratory. His current research interests are in wireless communications, nano-scale and molecular communications, and information theory. He is an Associate Editor of IEEE Transactions on Vehicular Technology, International Journal of Communication Systems (Wiley), and Nano Communication Networks Journal (Elsevier). He is currently General Co-Chair of ACM MOBICOM 2012, IEEE MoNaCom 2012, and TPC Co-Chair of IEEE ISCC 2012.